

Scaling Transformation for Free Convection Flow of a Micropolar Fluid along a Moving Vertical Plate in a Porous Medium with Velocity and Thermal Slip Boundary Conditions

Transformasi Penskalaan untuk Aliran Olakan Bebas Bendalir Mikropolar Sepanjang Plat Menegak dalam Medium Berliang dengan Syarat Sempadan Slip Halaju dan Haba

A.A. MUTLAG*, MD. JASHIM UDDIN & AHMAD IZANI MD. ISMAIL

ABSTRACT

We study and discuss the effect of thermal slip on steady free convection flow of a viscous, incompressible micropolar fluid past a vertical moving plate in a saturated porous medium. The effect of viscous dissipation is incorporated in the energy equation. The associated partial differential equations are transformed into a system of ordinary differential equations using similarity transformations generated by a group method and this system is then solved numerically. The effect of controlling parameters on the dimensionless velocity, angular velocity and temperature as well as friction factor, couple stress factor and heat transfer rate are shown graphically and discussed in detail. It is found that the dimensional velocity and angular velocity decrease whilst the temperature increases with velocity slip parameter. It is further found that thermal slip decreases the dimensional velocity and temperature but increases the dimensional angular velocity. Data from published work and our results are found to be in good agreement.

Keywords: Free convection; micropolar fluid; moving plate; porous medium; scaling group; velocity and thermal slip boundary conditions

ABSTRAK

Kami mengkaji dan membincangkan kesan slip haba pada aliran olakan bebas tak mampat bendalir mikro-kutub likat yang mantap melalui plat menegak yang bergerak dalam medium berliang tepu. Kesan penghambaran likat dimasukkan dalam persamaan tenaga. Persamaan pembezaan separa bersekutu dijelmakan kepada sistem persamaan pembezaan biasa menggunakan penjelmaan keserupaan yang dijanakan menggunakan kaedah kumpulan dan sistem ini kemudiannya diselesaikan secara berangka. Kesan parameter pengawal halaju tak berdimensi, halaju sudut dan suhu serta faktor geseran, faktor regangan pasangan dan kadar pemindahan haba ditunjukkan secara grafik dan dibincangkan secara terperinci. Didapati bahawa halaju berdimensi dan halaju sudut menurun manakala suhu naik dengan slip halaju. Adalah selanjutnya didapati bahawa slip haba menurun halaju berdimensi dan suhu tetapi meningkatkan halaju sudut berdimensi. Data daripada kerja yang telah diterbitkan dan keputusan kami didapati mempunyai persamaan.

Kata kunci: Bendalir mikropolar; kumpulan penskalaan; medium berliang; perolakan bebas; plat bergerak; syarat sempadan slip termal halaju dan termal

INTRODUCTION

Micropolar fluids are fluids with microstructure belonging to a class of non-Newtonian fluids with nonsymmetrical stress tensor. Physically, they represent fluids consisting of randomly oriented particles suspended in a viscous medium (Lukaszewicz 1999). According to previous researchers, liquid crystals, colloidal fluids, polymeric suspension and animal blood are some examples of micropolar fluids. Researchers have conducted research on micropolar fluids due to their diverse engineering applications ranging from biofluid mechanics of blood vessels to sediment transport in rivers and lubrication technology. In addition, micropolar fluids have applications in the development of micropolar biomechanical flows. Hydrodynamics of micropolar fluids have important applications variety of fields in physics and

engineering. Examples include synovial lubrication, knee cap mechanics, arterial blood flows, and cardio-vascular flows, cervical flows (spermatozoa propulsion dynamics), pharmacodynamics, drug delivery and peristaltic transport of micropolar fluid pumping (Reena & Rana 2009).

The theory of micropolar fluid was proposed by Eringen (1972, 1966). After the pioneering work of Eringen (1966), many researchers have studied micropolar fluid flow over various geometries subject to various boundary conditions. Some relevant studies include: Ishak et al. (2006) who considered steady laminar magnetohydrodynamic (MHD) boundary layer flow past a wedge with constant surface heat flux which is immersed in an incompressible micropolar fluid in the presence of a variable magnetic field; Hayat et al. (2009) who studied

MHD stagnation-point flow of an incompressible micropolar fluid over a nonlinear stretching surface; Sajid et al. (2009) found the exact solutions for thin film flows of a micropolar fluid and Rahman et al. (2010) who studied the heat transfer process in a two-dimensional steady hydromagnetic natural convective flow of a micropolar fluid over an inclined permeable plate which is subjected to a constant heat flux condition. In addition, free convection boundary layer flow of a micropolar fluid near a vertical permeable cone which has variable wall temperature was studied by Cheng (2011). Beg et al. (2011) presented an analysis for the steady free convection heat and mass transfer from a spherical body in a micropolar fluid. Rosali et al. (2012) analyzed the flow of micropolar fluid past a permeable stretching/shrinking sheet in a porous medium. Ahmad et al. (2012) have numerically studied the steady mixed convection boundary layer in laminar film flow of a micropolar fluid and Uddin et al. (2012a) studied the heat mass transfer for combined convective slips flow using Lie group.

In recent years, considerable attention has been devoted to the study of heat transfer and boundary layer flow characteristics in porous medium because of its extensive applications in engineering processes. Micropolar fluid flow through a porous medium has many applications, such as porous rocks, foams and foamed solid, aerogels, alloys, polymer blends and micro emulsions (Ingham & Pop 2005; Nield & Bejan 2006). Nadeem et al. (2010) examined the unsteady MHD boundary layer flow of a micropolar fluid through a porous medium. Mukhopadhyay (2011) observed that the heat transfer from the sheet to the fluid increases more slowly with the increase of the thermal slip parameter. Bhattacharyya et al. (2011) have shown that the heat transfer decreases with increasing thermal slip parameter whereas the temperature decreases.

Free convection flow occurs in various situations which includes atmospheric and oceanic circulation, electronic machinery, heated or cooled enclosures. Heat transfer by free convection in a porous medium has many important engineering and geophysical applications and a survey has been made by Bejan and Khair (1985), Ingham and Pop (2005), Nield and Bejan (2006) and Trevisan and Bejan (1990).

The objective of this paper was to extend the work of Ishak et al. (2006) for free convection flow in porous media and to include velocity and thermal slip effect. We apply the combined group similarity-numerical analysis technique and study the effect of the controlling parameters on the flow field and heat transfer characteristics as well as friction factor, couple stress factor and heat transfer rate. The present study may be applicable for micropolar fluid flows around microelectromechanical system.

MODELING OF TRANSPORT EQUATIONS

A steady 2-D viscous, incompressible micropolar fluid is assumed to flow along a moving vertical plate which moves with a constant velocity U_w (Figure 1). We suppose that the constant temperature of the wall is T_w and that of the

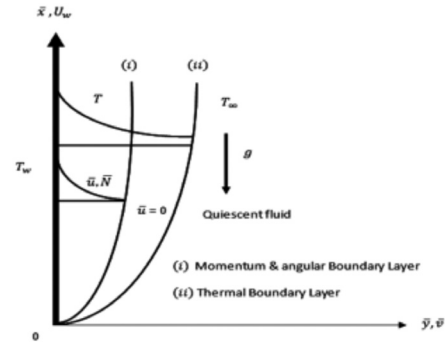


FIGURE 1. Flow configuration and coordinate system

surrounding fluid is T_∞ . It is assumed that $T_w > T_\infty$ (i.e. plate is heated). We incorporate the viscous dissipation term in the energy equation. The governing transport equations in dimensional form are (Ishak et al. 2006; Rosali et al. 2012

$$\frac{\partial \bar{u}}{\partial \bar{x}} + \frac{\partial \bar{v}}{\partial \bar{y}} = 0. \quad (1)$$

$$\bar{u} \frac{\partial \bar{u}}{\partial \bar{x}} + \bar{v} \frac{\partial \bar{u}}{\partial \bar{y}} = \left(\frac{\mu + k}{\rho} \right) \frac{\partial^2 \bar{u}}{\partial \bar{y}^2} + g\beta(T - T_\infty) + \frac{k}{\rho} \frac{\partial \bar{N}}{\partial \bar{y}} - \frac{\nu}{k_p} \bar{u}. \quad (2)$$

$$\bar{u} \frac{\partial \bar{N}}{\partial \bar{x}} + \bar{v} \frac{\partial \bar{N}}{\partial \bar{y}} = \frac{\gamma}{\rho j} \frac{\partial^2 \bar{N}}{\partial \bar{y}^2} - \frac{k}{\rho j} \left(2\bar{N} + \frac{\partial \bar{u}}{\partial \bar{y}} \right). \quad (3)$$

$$\bar{u} \frac{\partial T}{\partial \bar{x}} + \bar{v} \frac{\partial T}{\partial \bar{y}} = \alpha \frac{\partial^2 T}{\partial \bar{y}^2} + \left(\frac{\mu + k}{c_p \rho} \right) \left(\frac{\partial \bar{u}}{\partial \bar{y}} \right)^2. \quad (4)$$

The boundary conditions are (Bhattacharyya et al. 2011; Uddin et al. 2012a)

$$\begin{aligned} \bar{u} &= U_w + N_1(\bar{x})\nu \frac{\partial \bar{u}}{\partial \bar{y}}, \quad \bar{v} = 0, \quad N = -n \frac{\partial \bar{u}}{\partial \bar{y}}, \\ T &= T_\infty + D_1(\bar{x}) \frac{\partial T}{\partial \bar{y}} \quad \text{at } \bar{y} = 0, \\ \bar{u} &= 0, \quad \bar{N} = 0, \quad T = T_\infty \quad \text{as } \bar{y} \rightarrow \infty. \end{aligned} \quad (5)$$

Here (\bar{u}, \bar{v}) is the velocity components along axes, \bar{N} is the micro-rotation or angular velocity, ρ is the fluid density, c_p is the specific heat, ν is the kinematic viscosity, T is the temperature, k is the micro-polar vortex viscosity, β is the thermal volume expansion, μ is the dynamic viscosity, g is the acceleration due to gravity, j is the micro-inertia density, α is the thermal diffusivity and n is the a constant ($0 < n \leq 1$). The case $n = \frac{1}{2}$ indicates vanishing of anti-symmetrical part of the stress tensor and denotes weak concentration (Ishak et al. 2006), k_p is the permeability of the porous medium, g is the micropolar spin gradient viscosity, D_1 is the thermal slip factor and N_1 is the velocity slip factor.

NONDIMENSIONALIZATION

Introducing the following normalized variables (Ali et al. 2010)

$$x = \frac{\bar{x}}{L}, \quad y = \frac{\bar{y}}{L} \sqrt{\text{Re}}, \quad u = \frac{\bar{u}}{U_w}, \quad v = \frac{\bar{v}}{U_w} \sqrt{\text{Re}},$$

$$N = \frac{\bar{N}L}{U_w \sqrt{\text{Re}}}, \quad \theta = \frac{T - T_\infty}{T_w - T_\infty}, \quad \text{Re} = \frac{U_w L}{\nu}, \quad (6)$$

and the stream function ψ defined by $u = \partial\psi/\partial x$ and $v = -\partial\psi/\partial y$ into (2)- (5), give as

$$\frac{\partial\psi}{\partial y} \frac{\partial^2\psi}{\partial x \partial y} - \frac{\partial\psi}{\partial x} \frac{\partial^2\psi}{\partial y^2} = \left(\frac{\mu + k}{\rho} \right) \frac{\text{Re}}{U_w L} \frac{\partial^3\psi}{\partial y^3}$$

$$+ \frac{Lg\beta\Delta T}{U_w^2} \theta + \frac{\text{Re}}{U_w L} \frac{k}{\rho} \frac{\partial N}{\partial y} - \frac{\nu}{k_p} \frac{L}{U_w} \frac{\partial\psi}{\partial y}, \quad (7)$$

$$\frac{\partial\psi}{\partial y} \frac{\partial N}{\partial x} - \frac{\partial\psi}{\partial x} \frac{\partial N}{\partial y} = \frac{\text{Re}}{LU_w} \frac{\gamma}{\rho j} \frac{\partial^2 N}{\partial y^2} - \frac{kL}{\rho j U_w} \left(2N + \frac{\partial^2\psi}{\partial y^2} \right), \quad (8)$$

$$\frac{\partial\psi}{\partial y} \frac{\partial\theta}{\partial x} - \frac{\partial\psi}{\partial x} \frac{\partial\theta}{\partial y} = \frac{\alpha \text{Re}}{U_w L} \frac{\partial^2\theta}{\partial y^2} + \frac{U_w \text{Re}}{L\Delta T} \left(\frac{\mu + k}{c_p \rho} \right) \left(\frac{\partial^2\psi}{\partial y^2} \right)^2, \quad (9)$$

subject to the boundary conditions

$$\frac{\partial\psi}{\partial y} = 1 + N_1(x) \nu \frac{\sqrt{\text{Re}}}{L} \frac{\partial u}{\partial y}, \quad \frac{\partial\psi}{\partial x} = 0, \quad N = -n \frac{\partial^2\psi}{\partial y^2},$$

$$\theta = 1 + D_1(x) \frac{\text{Re}^{\frac{1}{2}}}{L} \frac{\partial\theta}{\partial y} \quad \text{at } y = 0, \quad (10)$$

$$\frac{\partial\psi}{\partial y} = 0, \quad N = 0, \quad \theta = 0 \quad \text{as } y \rightarrow \infty.$$

GROUP ANALYSIS AND INVARIANT TRANSFORMATIONS

We define the following scaling group of transformations which is a special form of Lie group (Mutlag et al. 2013; Uddin et al. 2012b)

$$\Gamma : x = e^{\varepsilon c_1} x^*, \quad y = e^{-\varepsilon c_2} y^*, \quad \psi = e^{-\varepsilon c_3} \psi^*, \quad \theta = e^{-\varepsilon c_4} \theta^*,$$

$$N = e^{-\varepsilon c_5} N^*, \quad \beta = e^{-\varepsilon c_6} \beta^*, \quad k_p = e^{-\varepsilon c_7} k_p^*, \quad D_1 = e^{-\varepsilon c_8} D_1^*, \quad (11)$$

$$j = e^{-\varepsilon c_9} j^*, \quad \gamma = e^{-\varepsilon c_{10}} \gamma^*, \quad N_1 = e^{-\varepsilon c_{11}} N_1^*.$$

Here ε is the parameter of the group Γ and $c_i^i S$, ($i = 1, 2, \dots, 11$) are arbitrary real numbers not all simultaneously zero. Equations (7)- (10) will remain invariant under the group of transformations in (11) if c_i hold following relationship

$$c_1 = c_7 = c_9 = c_{10} = 2c_1, \quad c_3 = c_8 = c_{11} = c_2,$$

$$c_4 = 0, \quad c_5 = -c_2, \quad c_6 = -2c_2. \quad (12)$$

Following Mutlag et al. (2013) and Uddin et al. (2012), we have the following invariants:

SIMILARITY TRANSFORMATIONS

$$\eta = \frac{1}{\sqrt{2x}} y, \quad \psi = \sqrt{2x} f(\eta), \quad \theta = \theta(\eta), \quad N = \frac{1}{\sqrt{2x}} h(\eta),$$

$$\beta = \frac{\beta^\circ}{x}, \quad k_p = x k_{p^\circ}, \quad D_1 = \sqrt{x} D_{1^\circ}, \quad j = x j^\circ, \quad \gamma = x \gamma^\circ, \quad N_1 = \sqrt{x} N_{1^\circ}, \quad (13)$$

where $\beta^\circ, k_{p^\circ}, D_{1^\circ}, j^\circ, \gamma^\circ, N_{1^\circ}$ are constant thermal volume expansion, permeability medium, thermal slip factor, microinertia density, the micropolar spin gradient viscosity and velocity slip factor, η is the similarity independent variable, $f(\eta)$ is the stream function, $\theta(\eta)$ is a temperature and $h(\eta)$ is angular velocity.

VERIFICATION OF OUR GROUP ANALYSIS

It is noticed that in the absence of buoyancy and Darcy terms and in the case of no slip boundary conditions, the similarity transformations (13) obtained by scaling group of transformations are consistent with the similarity transformations reported in Ishak et al. (2006). This validates our group analysis and invariant transformations.

GOVERNING SIMILARITY SOLUTIONS

Substituting (13) into (7)- (9), we get

$$(1 + \Delta) f''' + ff'' + \Delta h' + Gr \theta - 2Kf' = 0, \quad (14)$$

$$\lambda h'' + h'f + hf' - 2I(2h + f'') = 0, \quad (15)$$

$$\theta'' + \text{Pr} f\theta' + \text{Pr} Ec(1 + \Delta) f'^2 = 0. \quad (16)$$

The boundary conditions (10) become:

$$f'(0) = 1 + \delta f''(0), \quad f(0) = 0,$$

$$h(0) = -\eta f''(0), \quad \theta(0) = 1 + S \theta'(0),$$

$$f'(\infty) = h(\infty) = \theta(\infty) = 0 \quad (17)$$

The controlling parameters are: $\Delta = k/\mu$ (micropolar), $Gr = 2Lg \beta^\circ \Delta T / U_w^2$ (Grashof number), $K = \nu L / k_{p^\circ} U_w$ (permeability), $\lambda = \gamma^\circ / \rho \nu j^\circ$ (microrotational density), $I = Lk / \rho j^\circ U_w$ (vortex viscosity), $Ec = U_w^2 / c_p \Delta T$ (Eckert number), $\text{Pr} = \nu / \alpha$ (Prandtl number), $S = \sqrt{\text{Re}/2} D_{1^\circ} / L$ (thermal slip) and (velocity slip).

QUANTITIES OF PRACTICAL INTEREST

The physical quantities, the friction factor and rate of heat transfer are given by

$$C_{f,x} \sqrt{\text{Re}_x} = -\frac{1}{\sqrt{2}} [1 + \Delta(1 - n)] f''(0), \quad \frac{Nu_x}{\sqrt{\text{Re}_x}} = \frac{-1}{\sqrt{2}} \theta'(0), \quad (18)$$

where $\text{Re}_x = U_w \bar{x} / \nu$, is a local Reynolds number.

NUMERICAL SOLUTION AND VERIFICATIONS

Equations (14)-(16) along with the boundary condition in (17) were solved numerically using maple dsolve command with numeric option which uses the Runge-Kutta-Fehlberg fourth fifth (RKF45) order numerical method for solving two-point boundary value problem. RKF45 is a well-established adaptive numerical method for solving system of ordinary differential equations with

associated conditions (Butcher 2008) which uses both a fifth and a fourth order Runge-Kutta. The error of the Runge-Kutta Fehlberg algorithm is estimated and can be used for adaptive step sizing. The update formula for the fifth-fourth order Runge-Kutta Fehlberg algorithm is shown as follows.

$$\begin{aligned}
 k_0 &= f(x_i, y_i), \\
 k_1 &= f\left(x_i + \frac{1}{4}h, y_i + \frac{1}{4}hk_0\right), \\
 k_2 &= f\left(x_i + \frac{3}{8}h, y_i + \left(\frac{3}{32}k_0 + \frac{9}{32}k_1\right)h\right), \\
 k_3 &= f\left(x_i + \frac{12}{13}h, y_i + \left(\frac{1932}{2197}k_0 - \frac{7200}{2197}k_1 + \frac{7296}{2197}k_2\right)h\right), \\
 k_4 &= f\left(x_i + h, y_i + \left(\frac{439}{216}k_0 - 8k_1 + \frac{3860}{513}k_2 - \frac{845}{4140}k_3\right)h\right), \\
 k_5 &= f\left(x_i + \frac{1}{2}h, y_i + \left(-\frac{8}{27}k_0 + 2k_1 - \frac{3544}{2565}k_2 + \frac{1859}{4104}k_3 - \frac{11}{40}k_4\right)h\right), \\
 y_{i+1} &= y_i + \left(\frac{25}{216}k_0 + \frac{1408}{2565}k_2 + \frac{2197}{4104}k_3 - \frac{1}{5}k_4\right)h, \\
 z_{i+1} &= z_i + \left(\frac{16}{135}k_0 + \frac{6656}{12825}k_2 + \frac{28561}{56430}k_3 - \frac{9}{50}k_4 + \frac{2}{55}k_5\right)h,
 \end{aligned}
 \tag{19}$$

where y is a fourth-order Runge-Kutta and z is a fifth-order Runge-Kutta. An estimate of the error can be obtained by subtracting the two values obtained. If the error exceeds a specified threshold, the results can be recalculated using a smaller step size. The approach to estimate the new step size is:

$$h_{new} = h_{old} \left(\varepsilon h_{old} / 2 |z_{i+1} - y_{i+1}| \right)^{1/4}. \tag{20}$$

The step size is taken as $\Delta\eta = 0.001$ and the convergence criterion was set to 10^{-6} . The asymptotic boundary conditions given by (17) were replaced by using a value of 12 for the similarity variable η_{max} as follows.

$$\eta_{max} = 12, f'(12) = \theta(12) = h(\infty) = 0. \tag{21}$$

The choice of $\eta_{max} = 12$ ensured that all numerical solutions approached the asymptotic values correctly. Compilation times are of the order of several minutes on a PC.

VERIFICATION OF OUR NUMERICAL RESULTS

The numerical solutions were carried out for various values of the controlling parameters. The comparison of our present results with Ishak et al. (2006) showed excellent 10 agreement (Table 1). It is found from Table 1 that the skin friction factor is higher in the case of Newtonian fluids ($\Delta = 0$) than that of micropolar fluids. The reason is that micropolar fluids have greater resistance (resulting from dynamic viscosity and vortex viscosity) than Newtonian fluid.

TABLE 1. Values of $-f''(0)$ for different Δ with $Gr = K = S = \delta = 0, n = 0.5, Pr = 0.71, I = \lambda = Ec = 1$

Δ	Ishak et al. (2006)	Present study
0.0	0.6276	0.62757
0.5	0.5704	0.56118
1.0	0.5217	0.51204
2.0	0.4523	0.44311
4.0	0.3694	0.36202

RESULTS AND DISCUSSION

Table 2 shows the variation of the skin friction factor, the rate of heat transfer and the couple stress factor with the controlling parameters λ, I and S . It is observed that the skin friction factor reduces with λ and increases with I and S . It is further noticed from the same Table that heat transfer rates reduces with λ, I and S .

TABLE 2. Values of $-f''(0), -\theta'(0)$ and $-h'(0)$ for different λ, S and I with $K = n = 1, \Delta = 0.5, Gr = 0.3, Pr = 0.71, Ec = 0.1, \delta = 0$

λ	S	I	$-f''(0)$	$-\theta'(0)$	$-h'(0)$
0.5	0.5	1	1.42687	0.27793	2.41809
		1	1.39479	0.27594	1.79783
		1.5	1.37472	0.27514	1.50871
	0	0.2	1.26715	0.33643	0.54519
		0.1	1.27155	0.33643	0.54764
		0.5	1.28601	0.27555	0.55568
	1.5	0	1.22912	0.20817	0.03565
		0.5	1.350621	0.20243	0.94835
		1	1.384695	0.20262	1.35855

Figure 2 shows the variation of the skin friction factor, rate of heat transfer and couple stress factor with Δ and K . Figure 2(a) shows that the skin friction factor increases with increasing K . Figure 2(a) shows that the skin friction factor decreases with increasing of Δ . The reason increasing Δ implies decreasing viscosity μ which causes to increase velocity and hence reduces friction factor. Here $f''(0)$ is always negative, which implies that the plate exerts a drag force on the fluid. We also observe from Figure 2(b) that the rate of heat transfer decreases with K . Note that heat transfer rates for Newtonian fluid ($\Delta = 0$) is higher than that of micropolar fluid. A similar conclusion is also drawn by El-Aziz (2013). Here $-\theta'(0)$ is always positive, which implies that the heat is transferred from the hot sheet to the cold fluid. The couple stress factor increases with K (Figure 2(c)). All physical quantities decrease with Δ (Figure 2). This is because as Δ increases, all three boundary layer thickness become thicker.

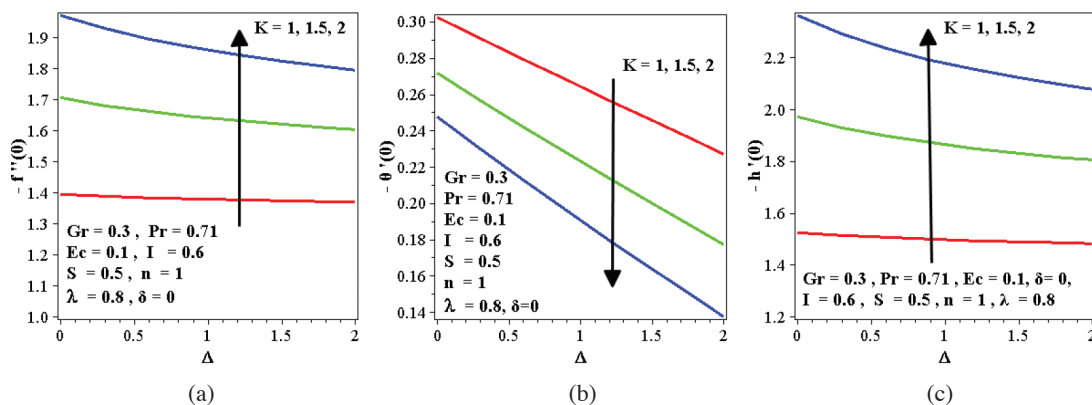


FIGURE 2. Effects of Δ and K on (a) friction factor, (b) Nusselt number and (c) the couple stress factor

Figure 3 shows the variation of the skin friction factor, rate of heat transfer and couple stress factor with Ec and δ . Figure 3(a) shows that the skin friction factor decreases with increasing δ . The boundary conditions (17) connecting slip velocity and friction factor shows that $f''(0) = \frac{f'(0)-1}{\delta}$. From this expression it is clear that friction factor decreases as slip parameter increases. We also observe from Figure 3b that the rate of heat transfer increases with δ . This is because increasing δ causes a greater amount of fluid to flow through the boundary layer due to the slipping effect. From the definition of Eckert number, $Ec > 0$ for $T_w > T_\infty$ (heated plate) and $Ec < 0$ for cooled plate ($T_w < T_\infty$). In our study we considered $Ec > 0$. All physical quantities decrease with the viscous dissipation parameter Ec . Recently, a similar conclusion is also drawn by El-Aziz (2013). The couple stress factor decreases with δ (Figure 3c).

Figure 4 shows the variation of Grashof number Gr on the velocity, temperature and angular velocity profiles. It is seen from Figure 4(a) that there is a rise in the velocity profiles with the increasing of Gr . Physically higher Gr values mean stronger convective currents which therefore enhance flow velocities in the porous medium. It is observed from Figure 4(b) that the temperature of the

fluid decreases when Gr increases. Physically, higher Gr values mean more heat is convected away from the plate to the fluid and hence temperatures decrease. Angular velocity is found to decrease with Gr (Figure 4(c)).

The effect of the permeability parameter K on the temperature and angular velocity profiles is displayed in Figure 5. It is noticed from Figure 5(a) that temperature increases significantly as K increases from 0 to 2, i.e. from high permeability to low permeability. The reason is increasing permeability reduces the presence of solid particles in the porous medium and hence raises temperature. It is noticed from Figure 5(b) that angular velocity also enhances significantly as K rises from 0 (high permeability) to 2 (low permeability). All angular velocity profiles have different values at the wall ($\eta = 0$). This is because of the boundary condition $h(0) = -nf''(0)$. As $n = 1$, h , is always nonzero since $f''(0) \neq 0$. The maximum microrotation at the wall occurs for the lowest permeability, where (approx.). Note that for high permeability ($K = 0$), $h(0)$, becomes negative i.e. -0.25 which implies reversal in spin. Hence, higher permeability materials may be used to reduce microrotational effects in suspension fluids.

Figure 6(a) shows that angular velocity rises with λ . The effect of n on the angular velocity is shown in

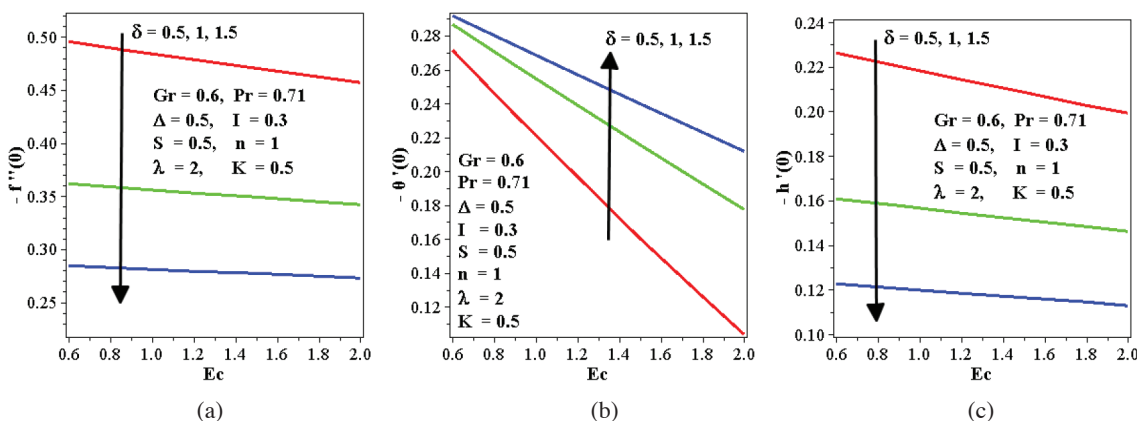


FIGURE 3. Effects of Ec and δ on (a) friction factor, (b) Nusselt number and (c) the couple stress factor

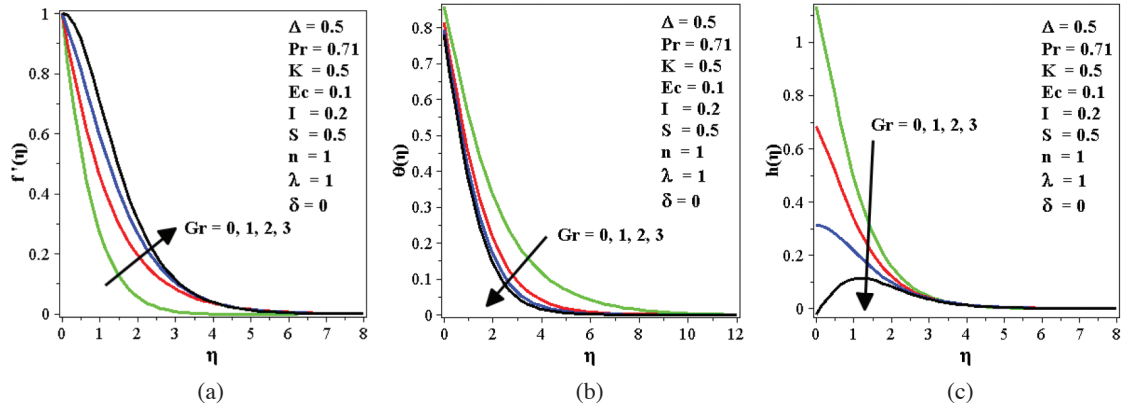


FIGURE 4. Effects of Gr on (a) velocity, (b) temperature and (c) angular velocity profiles

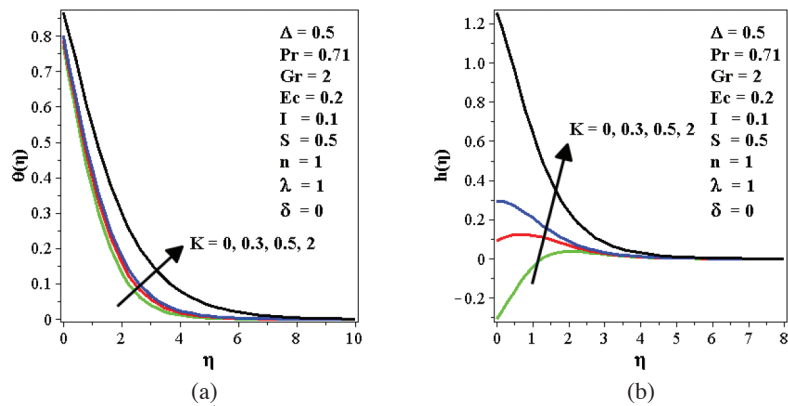


FIGURE 5. Effects of K on dimensionless (a) temperature and (b) angular velocity

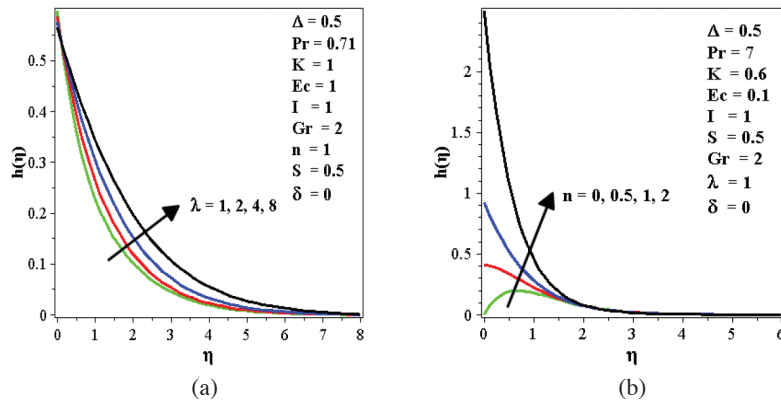


FIGURE 6. Variation of dimensionless angular velocity profile with (a) λ and (b) n

Figure 6(b). Note that the parameter n is in the boundary condition (17) and physically it relates to the concentration of microelements at the wall. Note that $n = 0$ implies zero spin i.e. stagnant particle at the wall while $n = 0.3, 0.7, 1.0$ mean higher concentrations of microelements, respectively. It is clear that greater n value imply greater microrotation, as displayed in Figure 6(b).

The effect of the vortex viscosity parameter (I) on the dimensionless angular velocity is exhibited in Figure

7. The angular velocity increases with increasing value of I when $K < 1$ (Figure 7(a)). We also observe from Figure 7(b) that for $K > 1$, the dimensionless angular velocity reduces due to rising value of I .

Figure 8 shows the velocity, temperature and angular velocity profiles for various S . Velocity and temperature decrease when S increases. Physically, the fluid in the boundary layer will not sense the heating effects of the plate due to rising of S and less amount of heat will be transferred

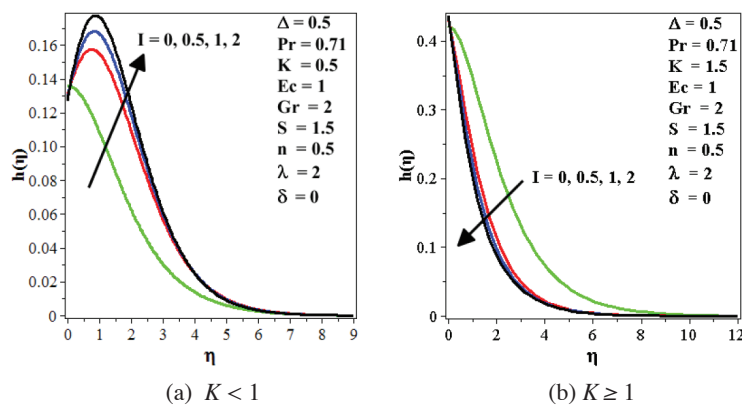


FIGURE 7. Dimensionless angular velocity profiles for different I

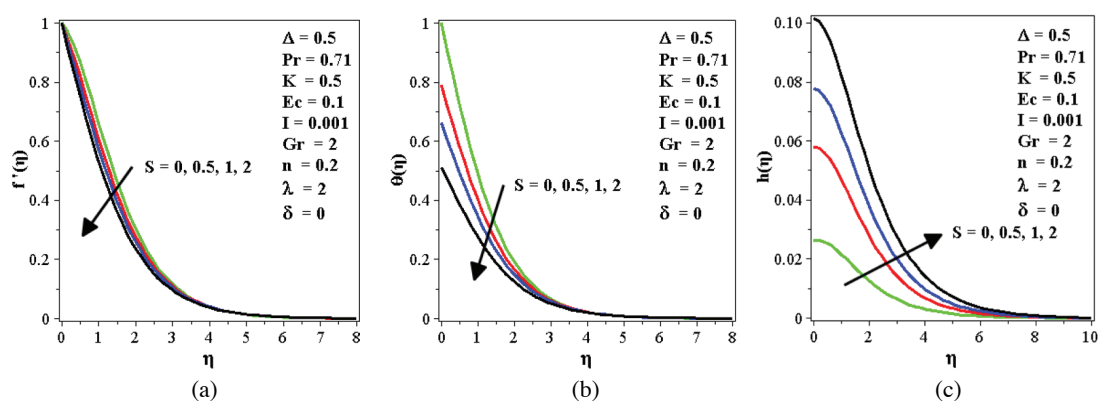


FIGURE 8. Effects of S on (a) velocity, (b) temperature and (c) angular velocity profiles

from the plate to the fluid and hence the velocity and temperature decrease. The opposite behavior for angular velocity is noticed (Figure 8(c)).

Figure 9 shows the variation of δ on velocity, temperature and angular velocity profiles. It is seen from Figure 9(a) that there is a reduction in the velocity profiles with the increasing of δ . It is clear that the maximum fluid dimensionless velocity at the wall is 1 when $\delta = 0$, which presents the conventional no-slip case. As the velocity slipping parameter δ increases, the differences between the wall and the fluid velocities near the wall increase. Again, it is clear that as the slipping parameter increases, the thickness of the velocity boundary layer decreases. Increasing the slipping factor may be looked at as a miscommunication between the source of motion (the plate) and the fluid domain. It is clear that hydrodynamic behavior of the problem under consideration is more sensitive to the variations in small values of δ as compared with the variations in large values of δ . Figure 9(b) shows that as the velocity slip parameter δ increases, less flow will be induced close to the plate layer and hence the hot plate heats a lesser amount of fluid and this causes higher increases in the fluid temperature. The boundary conditions in (17) shows that the effect of velocity slip on the angular velocity is indirect through the term $h(0) = -nf''(0)$. It is found that angular velocity reduces as δ increases (Figure

9(c)). Mathematically as δ increases $f''(0)$ decreases which causes the decrease in h . Finally, Figure 10 shows the effect of Eckert number which arises in high-speed aerodynamic flows, on the velocity, temperature and angular velocity. The viscous dissipation characterizes by the Eckert number produces heat due to drag between the fluid particles and this extra heat leads to an increase of the fluid temperature (Figure 10(b)). This increase of temperature leads to an increase of the buoyant force which in turn increases the velocity. It is found that the angular velocity decreases with the increase of Ec . In all cases we have considered positive Ec values i.e. heat is transferred from the sheet surface to the fluid by convection currents.

CONCLUSION

The effect of thermal slip and viscous dissipation on free convection flow of micropolar fluid past a semi-infinite moving vertical plate is investigated numerically. The similarity solutions are developed using scaling group transformation. The skin friction factor and the couple stress factor increase with increasing of K and decrease with increasing of Δ , Ec , δ . The rate of heat transfer decreases with Δ , K , Ec and increases with δ . The velocity rises but the angular velocity and temperature decrease when Gr increases. K increases the angular velocity and

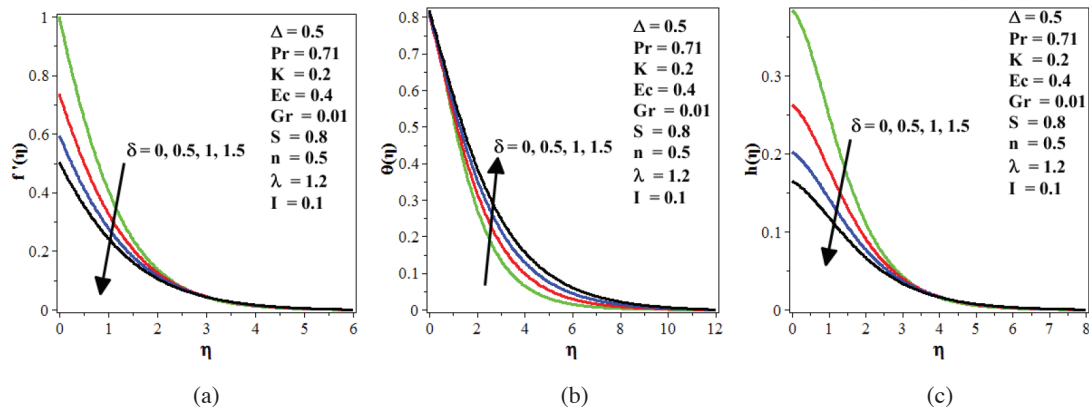


FIGURE 9. Effects of δ on (a) velocity, (b) temperature and (c) angular velocity profiles

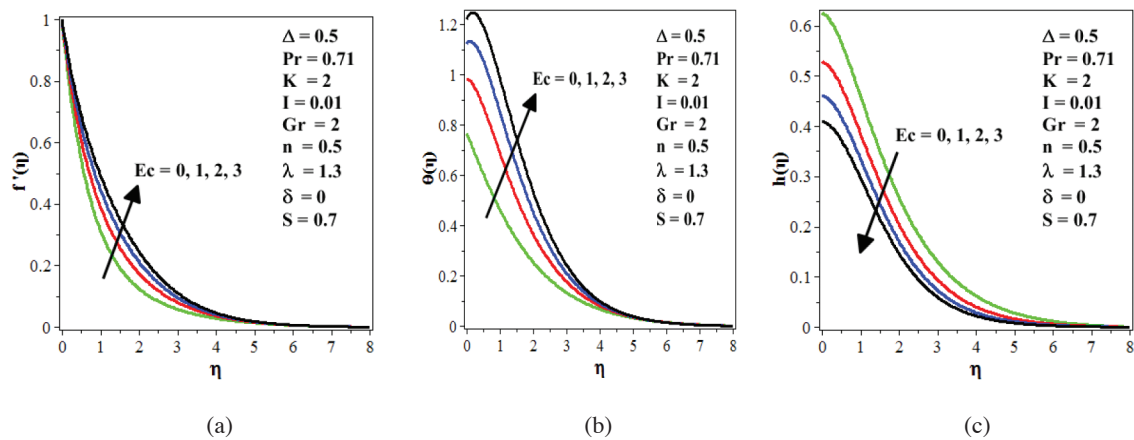


FIGURE 10. Effects of Ec on (a) velocity, (b) temperature and (c) angular velocity profiles

temperature. The angular velocity rises with λ and n . The dimensionless angular velocity increases with increasing value of I when $k < 1$ and for $k > 1$ the dimensionless angular velocity reduces due to rising value of I . The fluid velocity and temperature decrease while the angular velocity increases when S increases. The dimensionless velocity and the angular velocity decrease but temperature rises as δ increases.

ACKNOWLEDGMENTS

The authors acknowledge the financial support of USM.

REFERENCES

- Ahmad, K., Nazar, R. & Pop, I. 2012. Mixed convection in laminar film flow of a micropolar fluid. *International Communications in Heat and Mass Transfer* 39: 36-39.
- Ali, A., Amin, N. & Pop, I. 2010. Unsteady mixed convection boundary layer from a circular cylinder in a micropolar fluid. *International Journal of Chemical Engineering* 2010: 417875.
- Beg, O.A., Ramachandra Prasad, V., Vasu, B., Bhaskar Reddy, N., Li, Q. & Bhargava, R. 2011. Free convection heat and mass transfer from an isothermal sphere to a micropolar regime with Soret/Dufour effects. *International Journal of Heat and Mass Transfer* 54: 9-18.
- Bejan, A. & Khair, K.R. 1985. Heat and mass transfer by natural convection in a porous medium. *International Journal of Heat and Mass Transfer* 28: 909-918.
- Bhattacharyya, K., Mukhopadhyay, S. & Layek, G.C. 2011. Steady boundary layer slip flow and heat transfer over a flat porous plate embedded in a porous media. *Journal of Petroleum Science and Engineering* 78: 304-309.
- Butcher, J.C. 2008. *Numerical Methods for Ordinary Differential Equations*. England. John Wiley & Sons, Ltd.
- Cheng, C. 2011. Natural convection boundary layer flow of a micropolar fluid over a vertical permeable cone with variable wall temperature. *International Communications in Heat and Mass Transfer* 38: 429-433.
- El-Aziz, M.A. 2013. Mixed convection flow of a micropolar fluid from an unsteady stretching surface with viscous dissipation. *Journal of the Egyptian Mathematical Society* 21: 385-394.
- Eringen, A.C. 1966. Theory of micropolar fluids. *Journal of Mathematics and Mechanics* 16: 1-18.
- Eringen, A.C. 1972. Theory of thermomicropolar fluids. *Journal of Mathematical Analysis and Applications* 38: 480-496.
- Hayat, T., Javed, T. & Abbas, Z. 2009. MHD flow of a micropolar fluid near a stagnation-point towards a non-linear stretching surface. *Nonlinear Analysis: Real World Applications* 10: 1514-1526.
- Ingham, D.B. & Pop, I. 2005. *Transport Phenomena in Porous Media*. 3rd ed. Oxford, UK: Elsevier.

- Ishak, A., Nazar, R. & Pop, I. 2006. Flow of a micropolar fluid on a continuous moving surface. *Archives of Mechanics* 58: 529-541.
- Lukaszewicz, G. 1999. *Micropolar Fluids: Theory and Applications*. New York: Springer.
- Mukhopadhyay, S. 2011. Effects of slip on unsteady mixed convective flow and heat transfer past a porous stretching surface. *Nuclear Engineering and Design* 241: 2660-2665.
- Mutlag, A.A., Uddin, M.J., Hamad, M.A.A. & Ismail, A.I.M. 2013. Heat transfer analysis for falkner-skam boundary layer flow past a stationary wedge with slips boundary conditions considering temperature-dependent thermal conductivity. *Sains Malaysiana* 42: 855-862.
- Nadeem, S., Hussain, M. & Naz, M. 2010. MHD stagnation flow of a micropolar fluid through a porous medium. *Meccanica* 45: 869-880.
- Nield, D.A. & Bejan, A. 2006. *Convection in Porous Media*. 3rd ed. New York: Springer.
- Rahman, M.M., Aziz, A. & Al-Lawatia, M.A. 2010. Heat transfer in micropolar fluid along an inclined permeable plate with variable fluid properties. *International Journal of Thermal Sciences* 49: 993-1002.
- Reena & Rana, U.S. 2009. Effect of dust particles on rotating micropolar fluid heated from below saturating a porous medium. *Applications and Applied Mathematics* 4: 189-217.
- Rosali, H., Ishak, A. & Pop, I. 2012. Micropolar fluid flow towards stretching/shrinking sheet in a porous medium with suction. *International Communications in Heat and Mass Transfer* 39: 826-829.
- Sajid, M., Ali, N. & Hayat, T., 2009. On exact solutions for thin film flows of a micropolar fluid. *Communications in Nonlinear Science and Numerical Simulation* 14: 451-461.
- Trevisan, O.V. & Bejan, A. 1990. Combined heat and mass transfer by natural convection in a porous medium. *Advances in Heat Transfer* 20: 315-352.
- Uddin, M.J., Hamad, M.A.A. & Ismail, A.I.M. 2012a. Investigation of heat mass transfer for combined convective slips flow: A lie group analysis. *Sains Malaysiana* 41: 1145-1155.
- Uddin, M.J., Khan, W.A. & Ismail, A.I.M. 2012b. MHD free convective boundary layer flow of a nanofluid past a flat vertical plate with Newtonian heating boundary condition. *Plos One* 7: e49499.

A.A. Mutlag*, Md. Jashim Uddin & Ahmad Izani Md. Ismail
School of Mathematical Sciences
Universiti Sains Malaysia
11800 Penang
Malaysia

A.A. Mutlag*
Mathematics Department
College of Education for Pure Science
AL- Anbar University, ALAnbar
Iraq

Md. Jashim Uddin
Mathematics Department
American International University-Bangladesh
Banani Dhaka, 1213
Bangladesh

*Corresponding author; email: alassafi2005@yahoo.com

Received: 11 January 2013

Accepted: 9 December 2013